

# Noise-Augmented $\ell_0$ Regularization of Tensor Regression with Tucker Decomposition

Tian Yan\*, Yinan Li, Fang Liu†

Applied and Computational Mathematics and Statistics  
University of Notre Dame, Notre Dame, IN 46556, USA

## Abstract

Tensor data are multi-dimension arrays. Low-rank decomposition-based regression methods with tensor predictors exploit the structural information in tensor predictors while significantly reducing the number of parameters in tensor regression. We propose a method named  $\text{NA}_0\text{CT}^2$  (Noise Augmentation for  $\ell_0$  regularization on Core Tensor in Tucker decomposition) to regularize the parameters in tensor regression (TR), coupled with Tucker decomposition. We establish theoretically that  $\text{NA}_0\text{CT}^2$  achieves exact  $\ell_0$  regularization in linear TR and generalized linear TR on the core tensor from the Tucker decomposition. To our knowledge,  $\text{NA}_0\text{CT}^2$  is the first Tucker decomposition-based regularization method in TR to achieve  $\ell_0$  in core tensor.  $\text{NA}_0\text{CT}^2$  is implemented through an iterative procedure and involves two simple steps in each iteration – generating noisy data based on the core tensor from the Tucker decomposition of the updated parameter estimate and running a regular GLM on noise-augmented data on vectorized predictors. We demonstrate the implementation of  $\text{NA}_0\text{CT}^2$  and its  $\ell_0$  regularization effect in both simulation studies and real data applications. The results suggest that  $\text{NA}_0\text{CT}^2$  improves predictions compared to other decomposition-based TR approaches, with or without regularization and it also helps to identify important predictors though not designed for that purpose.

**keywords:** tensor regression (TR), low-rank decomposition, CP decomposition, Tucker decomposition, vectorization,  $\ell_0$  regularization, sparsity, noise augmentation, generalized linear model

## 1 Introduction

Tensor data are  $D$ -dimensional arrays in the  $\mathbb{R}^{I_1 \times I_2 \times \dots \times I_D}$  space. Many applications, such as medical imaging and recommendation systems, contain tensor data. Vectors are 1D tensors ( $D = 1$ ) and matrices are 2D tensors ( $D = 2$ ). A naïve approach for analyzing tensor data is

---

\*Tian Yan is supported by the China Scholarship Council.

†corresponding author (fang.liu.131@nd.edu)

to vectorize tensors and apply traditional regression models to the vectorized data. Not only do regression models on vectorized data involve a number of parameters in this approach, but the structural information contained in the original tensors also is not leveraged during the estimation. To overcome these limitations, tensor regression (TR) models are proposed by applying low-rank decomposition to tensors, including the CANDECOMP/PARAFAC (CP) decomposition (Harshman et al., 1970; Carroll and Chang, 1970) and the Tucker decomposition (Tucker, 1966), that would reduce the number of parameters in regression models (e.g. from tens of millions down to a few hundred (Zhou et al., 2013)) while retaining the spatial structure information in tensor data. Even with low-rank decomposition, the number of parameters ( $p$ ) in TR may still be large relative to the sample size ( $n$ ). When  $n < p$ , regularizations on TR parameters are necessary for the parameter to be identifiable; even if  $n > p$ , regularizations are often employed to improve the generalization of estimated TR.

Guo et al. (2011) apply CP decomposition in linear TR and regularize parameters with Frobenius norm and group-sparsity norm. Zhou et al. (2013) apply CP decomposition and suggest that commonly used regularizers for generalized linear models (GLMs) can be also applied to TR, such as the bridge, ridge, lasso, elastic net, and SCAD regularizers. Signoretto et al. (2014) extend spectral regularization to TR with convex and differentiable loss functions. Liu et al. (2014) impose Frobenius norm on the difference between a full tensor and its CP decomposition and trace norm on its CP components to achieve relaxed rank regularization and use alternating direction method of multipliers (ADMM) for optimization (Boyd et al., 2011). Wimalawarne et al. (2016) investigate regularization based on overlapped trace norm and (scaled) latent trace norm and employ dual optimization to estimate parameters. Song and Lu (2017) impose both nuclear and  $\ell_1$  norms in linear TR to achieve a mixture of rank and  $\ell_1$  regularization. Li et al. (2018) employ Tucker decomposition and regularize the core tensor with common regularizers for GLMs. Raskutti et al.

(2019) assume that tensor parameters are located in a low-dimensional subspace and convex and weakly decomposable (a relaxed regularity condition on regularizers to study their oracle properties; see van de Geer (2014) regularizers, and propose a convex optimization framework for multi-dimensional responses. The rank of a low-rank decomposition in TR is often assumed known or pre-specified. If the rank is unknown or not prespecified, the method by He et al. (2018) can be applied that assumes sparsity in each unit-rank tensor in CP decomposition and conducts unit-rank tensor regression iteratively. Ou-Yang et al. (2020) impose sparsity regularization on coefficient tensors directly rather than factor matrices from the CP decomposition of the former, and use ADMM for optimization. Roy and Michailidis (2022) decompose a coefficient tensor into a low tubal rank tensor and a sparse tensor and solve a convex optimization problem using ADMM. Chen et al. (2022) consider the correlation between different slices of a coefficient tensor, and propose latent F-1 norm that set an entire slice of the tensor at zero to promote sparsity. Xu et al. (2022) develop a graph regularizer to incorporate domain knowledge (intra-modal relations) in TR that is encoded in a graph Laplacian matrix and apply the approach to financial data.

Many of the methods mentioned above assume convexity on loss functions. Chen et al. (2019) propose a non-convex projected gradient descent algorithm with error bounds on estimated tensors and show superior performance in both statistical error and run-time in examples.  $\ell_0$  regularization is also non-convex. To our knowledge, there is little work that explores the  $\ell_0$  regularization in TR.  $\ell_0$  regularization is a desirable regularizer in that it sets zero-valued parameters exactly at zero while providing unbiased estimates for non-zero parameters. On the other hand,  $\ell_0$  regularization is NP-hard. In the setting of GLMs, approximate  $\ell_0$  regularizations through continuous functions are often used, such as Wei et al. (2018); Tang et al. (2014); Hyder and Mahata (2009); Liu and Li (2016); Dicker et al. (2013); Lv and Fan (2009); Shi et al. (2018), among others. Some of these methods are examined

only when the loss function is least squares and do not offer theoretical guarantees that the approximated  $\ell_0$  regularizations achieve both accurate variable selection and unbiased estimates for non-zero parameters, and some of them would require the development of new optimization procedures to achieve more efficient computation or more accurate results. To our knowledge, these approximate  $\ell_0$  regularizers have not been examined in TR with CP or Tucker decompositions.

In this study, we propose to achieve  $\ell_0$  regularization in TR using the noise-augmented (NA) regularization technique. NA has been used for regularizing the estimation and inferences in GLMs estimation and construction of single and multiple undirected graphs (Li et al., 2021; Li and Liu, 2022). It works by augmenting the original data with noisy samples drawn from Gaussian distributions with adaptive variance terms designed to achieve different types of regularizations such as the bridge, ridge, lasso, elastic net, SCAD, group lasso, as well as  $\ell_0$  regularizations among others. In this work, we design a noise term to achieve  $\ell_0$  regularization in TR with Tucker decomposition. Specifically,  $\ell_0$  regularization on the core tensor is achieved by promoting orthogonality between the elements in the core tensor and noisy data.

We refer to our method as  $NA_0CT^2$  (*Noise Augmentation for  $\ell_0$  regularization on Core Tensor in Tucker decomposition*). To our knowledge,  $NA_0CT^2$  is the first to explore the  $\ell_0$  regularization on the core tensor with the Tucker decomposition in TR. The achieved sparsity on the core tensor elements through  $NA_0CT^2$  help identify important variables that matter in the prediction and interpret high-dimensional TR models. In addition,  $NA_0CT^2$  is easy to implement and involves a simple noisy data generation step followed by running regular GLMs (without regularizers) on noise-augmented data iteratively, where one can leverage existing software.

In what follows, we first introduce some basic concepts on tensor decomposition and TR in

Section 2. We present the NA<sub>0</sub>CT<sup>2</sup> method and an algorithm to implement it in Section 3. We apply NA<sub>0</sub>CT<sup>2</sup> to both simulated tensor data and a real tensor dataset in Section 4. The paper concludes in Section 5 with some final remarks on NA<sub>0</sub>CT<sup>2</sup> and provides future research directions.

## 2 Preliminaries

Let  $x$  denote a scalar,  $\mathbf{x}$  denote a vector,  $\mathbf{X}$  denote a matrix, and  $\mathcal{X}$  denote a  $I_1 \times I_2 \times \cdots \times I_D$  tensor, where  $D$  is the dimensionality or the *order* of the tensor, the  $d$ -th dimension is known as the  $d$ -mode for  $d = 1, \dots, D$ , and  $I_d$  is the dimension of the  $d$ -mode. For example, a typical Magnetic Resonance Imaging (MRI) image is of size  $256 \times 256 \times 256$ . If expressed as a tensor, it is of order 3 and  $I_d = 256$  for  $d = 1, 2, 3$ . We use  $x_{i,j}$  to denote the element  $(i, j)$  in matrix  $\mathbf{X}$ , and  $x_i$  to denote element  $i$  in vector  $\mathbf{x}$ , and  $x_{i_1 i_2 \dots i_D}$  to denote the element in position  $(i_1, i_2, \dots, i_D)$  in  $\mathcal{X} \in \mathbb{R}^{I_1 \times I_2 \times \dots \times I_D}$ .

A tensor can be formulated as an *outer product* of  $D$  vectors as in  $\mathcal{X} = \mathbf{a}^{(1)} \circ \mathbf{a}^{(2)} \circ \cdots \circ \mathbf{a}^{(D)}$ , where  $\mathbf{a}^{(i)} \in \mathbb{R}^{I_i}$  for  $1 \leq i \leq D$ ; the element  $x_{i_1 i_2 \dots i_D}$  in  $\mathcal{X}$  is given by  $a_{i_1}^{(1)} a_{i_2}^{(2)} \dots a_{i_D}^{(D)}$  for  $1 \leq i_d \leq I_D$ . The *vectorization* of  $\mathcal{X} \in \mathbb{R}^{I_1 \times I_2 \times \dots \times I_D}$  is denoted by  $\text{vec}(\mathcal{X})$ , and  $x_{i_1 i_2 \dots i_D}$  is the  $(1 + \sum_{d=1}^D (i_d - 1) \prod_{d'=1}^{d-1} I_{d'})$ -th element of  $\text{vec}(\mathcal{X})$  (when  $d = 1$ ,  $\prod_{d'=1}^{d-1} I_{d'}$  is replaced by 1). The  $d$ -mode *matricization* of  $\mathcal{X} \in \mathbb{R}^{I_1 \times I_2 \times \dots \times I_D}$  is denoted as  $\mathbf{X}_{(d)} \in \mathbb{R}^{I_d \times (I_1 I_2 \dots I_{d-1} I_{d+1} \dots I_D)}$  and  $x_{i_1 i_2 \dots i_D}$  is entry  $(i_d, j)$  in matrix  $\mathbf{X}_{(d)}$ , where  $j = 1 + \sum_{k=1, k \neq d}^D (i_k - 1) \prod_{m=1, m \neq d}^{k-1} I_m$  (when  $k = 1$ ,  $\prod_{m=1, m \neq d}^{k-1} I_m$  is replaced by 1). The  $d$ -mode *product* of tensor  $\mathcal{X} \in \mathbb{R}^{I_1 \times I_2 \times \dots \times I_D}$  and matrix  $\mathbf{A} \in \mathbb{R}^{J \times I_d}$ , denoted by  $\mathcal{X} \times_d \mathbf{A} \in \mathbb{R}^{I_1 \times I_2 \times \dots \times I_{d-1} \times J \times I_{d+1} \times \dots \times I_D}$ , is given by  $(\mathcal{X} \times_d \mathbf{A})_{i_1 i_2 \dots i_{d-1} j i_{d+1} \dots i_D} = \sum_{i_d=1}^{I_d} x_{i_1 i_2 \dots i_D} a_{j i_d}$ . The *inner product* of two tensors  $\mathcal{X}$  and  $\mathcal{Y}$  of the same order  $D$  is  $\langle \mathcal{X}, \mathcal{Y} \rangle$  that is calculated as  $\sum_{i_1=1}^{I_1} \sum_{i_2=1}^{I_2} \cdots \sum_{i_D=1}^{I_D} x_{i_1 i_2 \dots i_D} y_{i_1 i_2 \dots i_D}$ .

In TR, predictors  $\mathcal{X}_i \in \mathbb{R}^{I_1 \times I_2 \times \dots \times I_D}$  are tensors and observations  $\mathbf{y} = (y_1, y_2, \dots, y_n)$  on response variable  $Y$  are assumed to be independently identically distributed. If  $Y$  belongs

to exponential family distributions, then TR models can be formulated as follows,

$$p(y_i|\mathcal{X}_i, \mathcal{B}, \phi) = \exp\left\{\frac{y_i\langle\mathcal{X}_i, \mathcal{B}\rangle - B(\langle\mathcal{X}_i, \mathcal{B}\rangle)}{a(\phi)} + h(y_i, \phi)\right\}, \quad (1)$$

where  $\mathcal{B} \in \mathbb{R}^{I_1 \times I_2 \times \dots \times I_D}$  contains unknown parameters and is a tensor of the same order as  $\mathcal{X}$ . The most straightforward way to run the model in Eqn (1) with a tensor predictor to vectorize  $\mathcal{X}$  and  $\mathcal{B}$  and run GLM with or without regularization on the vectorized  $\mathcal{B}$ . However, the number of parameters  $\prod_{i=1}^D I_i$  in  $\mathcal{B}$  is usually large, causing difficulty in both estimation and computation, as well as in the interpretability of the estimated model. In addition, the structural information in  $\mathcal{X}$  is lost. To reduce the number of parameters while retaining some structural information in the tensor data, TR can be run with a low-rank decomposition of  $\mathcal{B}$ , such as Tucker decomposition or the CP decomposition, instead of a fully-parameterized  $\mathcal{B}$ .

A *Tucker decomposition* of tensor  $\mathcal{B} \in \mathbb{R}^{I_1 \times I_2 \times \dots \times I_D}$  is defined as

$$\begin{aligned} \mathcal{B} &\approx \mathcal{G} \times_1 \mathbf{U}_1 \times_2 \mathbf{U}_2 \times_3 \dots \times_D \mathbf{U}_D = \llbracket \mathcal{G}; \mathbf{U}_1, \mathbf{U}_2, \dots, \mathbf{U}_D \rrbracket \\ &= \sum_{r_1=1}^{R_1} \sum_{r_2=1}^{R_2} \dots \sum_{r_D=1}^{R_D} g_{r_1 r_2 \dots r_D} \mathbf{u}_1^{r_1} \circ \mathbf{u}_2^{r_2} \circ \dots \circ \mathbf{u}_D^{r_D}, \end{aligned} \quad (2)$$

where  $\mathcal{G} \in \mathbb{R}^{R_1 \times R_2 \times \dots \times R_D}$  is the *core tensor* with  $R_d \leq I_d$ ,  $\mathbf{U}_d \in \mathbb{R}^{I_d \times R_d}$  is a matrix with orthonormal columns for  $d = 1, \dots, D$ , and  $\mathbf{u}_d^{r_d}$  is the  $r_d$ -th column of matrix  $\mathbf{U}_d$  for  $d = 1, \dots, D$ . When  $R_d = I_d$ , the Tucker decomposition in Eqn (2) is an exact representation of the original tensor and “ $\approx$ ” can be replaced by “ $=$ ”. When  $R_d < I_d$ , the core tensor is often viewed as a compressed representation of the original tensor. The Tucker decomposition can be regarded as a form of higher-order principal component analysis;  $\mathbf{U}_d$  is the “principle component” in the  $d$ -mode and the elements in the core tensor measure the relative importance of the principle components.

An rank- $R$  CP decomposition of  $\mathcal{B}$  is

$$\mathcal{B} \approx \llbracket \mathbf{g}; \mathbf{U}_1, \mathbf{U}_2, \dots, \mathbf{U}_D \rrbracket = \sum_{r=1}^R g_r \mathbf{u}_1^r \circ \mathbf{u}_2^r \circ \dots \circ \mathbf{u}_D^r, \quad (3)$$

where  $\mathbf{g} = (g_1, \dots, g_R) \in \mathbb{R}^R$ ,  $\mathbf{U}_d \in \mathbb{R}^{I_d \times R}$  for  $d = 1, \dots, D$ ,  $\|\mathbf{u}_d^r\|_2 = 1$ , and is the  $r$ -th column of matrix  $\mathbf{U}_d$ , and  $\mathbf{u}_d^r \in \mathbb{R}^{I_d}$  for  $d = 1, \dots, D$ . In other words,  $\mathcal{B}$  is the sum of  $R$  rank-one tensors of dimensions  $I_1, \dots, I_D$ , respectively. If  $\mathcal{B}$  can be expressed exactly as the sum of  $R$  rank-one tensors, then  $\mathcal{B}$  admits a rank  $R$  decomposition and “ $\approx$ ” in Eqn (3) can be replaced by “ $=$ ”. The CP decomposition can be regarded as a special case of the Tucker decomposition when the core tensor is super-diagonal and  $R_d$  in is the same for all  $d = 1, \dots, D$  Eqn (2). If we relax the requirement of  $\|\mathbf{u}_d^r\|_2 = 1$ ,  $g_r$  in Eqn (3) can be incorporated in any of the  $\mathbf{u}_d^r$  terms for  $d = 1, \dots, D$ . For example, if  $g_r$  is multiplied with  $\mathbf{u}_1$ , the CP decomposition can be written as  $\sum_{r=1}^R \mathbf{u}'_1 \circ \mathbf{u}_2^r \circ \dots \circ \mathbf{u}_D^r$ , where  $\mathbf{u}'_1 = \mathbf{g}_r \cdot \mathbf{u}_1^r$  (element-wise multiplication).

Applying the Tucker and CP compositions,  $\langle \mathcal{X}_i, \mathcal{B} \rangle$  in the TR model in Eq (2) can be written, respectively, as

$$\langle \mathcal{X}_i, \mathcal{B} \rangle = \langle \mathcal{X}_i, \llbracket \mathcal{G}; \mathbf{U}_1, \mathbf{U}_2, \dots, \mathbf{U}_D \rrbracket \rangle = \langle \mathcal{X}_i, \sum_{r_1=1}^{R_1} \sum_{r_2=1}^{R_2} \dots \sum_{r_D=1}^{R_D} g_{r_1 r_2 \dots r_D} \mathbf{u}_1^{r_1} \circ \mathbf{u}_2^{r_2} \circ \dots \circ \mathbf{u}_D^{r_D} \rangle, \quad (4)$$

$$\langle \mathcal{X}_i, \mathcal{B} \rangle = \langle \mathcal{X}_i, \llbracket \mathbf{g}; \mathbf{U}_1, \mathbf{U}_2, \dots, \mathbf{U}_D \rrbracket \rangle = \langle \mathcal{X}_i, \sum_{r=1}^R g_r \mathbf{u}_1^r \circ \mathbf{u}_2^r \circ \dots \circ \mathbf{u}_D^r \rangle. \quad (5)$$

$\mathcal{G}, \mathbf{g}, \mathbf{u}'$  will thus be estimated instead of the elements in the original tensor  $\mathcal{B}$ . As mentioned above, the model based on either of the two decompositions can lead to a potentially significant decrease in the number of parameters while honoring at least partially the structural information in  $\mathcal{B}$  compared to a GLM with vectorized  $\mathcal{B}$  and  $\mathcal{X}$ . Table 1 lists the numbers of free parameters in the original tensor  $\mathcal{B}$ , its Tucker decomposition, and its CP decomposition. For CP decomposition, the number of free parameters, compared to that in the original  $\mathcal{B}$ , would be much smaller. For example, For  $D = 3$  and  $I_d = 64$ , then the number of parameters

goes from 262,144 down to 6,080 if  $R = 32$  (97.7% decrease) and down to 12,160 if  $R = 64$  (95.3% decrease). In the case of Tucker decomposition,  $R_d$  needs to be smaller than  $I_d$  at least for some  $d$  in order for the number of free parameters to decrease from that in the original  $\mathcal{B}$ ; otherwise, the number of parameters would not be reduced though it still has the benefit of honoring the structural information in  $\mathcal{X}$  via the decomposition and provides more control over the what parameters to regularize in the model.

Table 1: Number of free parameters in Tucker decomposition and CP decomposition of tensor  $\mathcal{B} \in \mathbb{R}^{I_1 \times I_2 \times \dots \times I_D}$  (Li et al., 2018)

	rank- $R$ CP	Tucker	original
$D = 2$	$R(I_1 + I_2) - R^2$	$I_1 R_1 + I_2 R_2 + R_1 R_2 - R_1^2 - R_2^2$	$\prod_{d=1}^D I_d$
$D > 2$	$R(\sum_{d=1}^D I_d - D + 1)$	$\sum_{d=1}^D I_d R_d + \prod_{d=1}^D R_d - \sum_{d=1}^D R_d^2$	$\prod_{d=1}^D I_d$

### 3 Method

Though CP decomposition is simple, it is often limited in its approximation capability and requires  $\mathbf{u}_d^r$  to have the same dimension for any fixed  $d$  and different  $r$ , where  $r = 1, 2, \dots, R$  in 3. In Comparison, Tucker decomposition is more flexible and allows different numbers of components in different modes after the decomposition and as well as less structure on the core tensor (CP is a special case of Tucker with a super-diagonal structure for the core tensor). For this reason, we focus on TR decomposition. Interested readers may also refer to (Li et al., 2018) for the comparison between Tucker and CP decompositions when used in the TR setting.

We examine the case when response variable  $Y$  follows an exponential family distribution given in Eq (1). The loss function is the negative log-likelihood function of  $\mathcal{B}$  (other loss functions without making distributional assumptions, such as the simply  $\ell_2$  loss or cross-entropy loss, can be used as seen appropriate),

$$l = l(\mathcal{B}|\mathbf{y}, \mathcal{X}_i, 1 \leq i \leq n) = -\sum_{i=1}^n \ln p(y_i|\mathcal{X}_i, \mathcal{B}). \quad (6)$$



Our proposed method NA<sub>0</sub>CT<sup>2</sup> applies Tucker decomposition to  $\mathcal{B}$  (Eq (2)) and uses an iterative procedure to estimate the core tensor  $\mathcal{G}$  with  $\ell_0$  regularization and  $\mathbf{U}_d$  for  $d = 1, \dots, D$ . Each iteration  $t$  contains just two simple steps: generate noisy data  $(\mathcal{Z}_j^{(t)}, e_{y,j}^{(t)})$  for  $j = 1, \dots, n_e$  given the updated tensor estimate from iteration  $t - 1$ , and run GLM on the updated noise-augmented data

$$\begin{bmatrix} (\mathcal{X}_i, y_i)_{i=1, \dots, n} \\ (\mathcal{Z}_j^{(t)}, e_{y,j}^{(t)})_{j=1, \dots, n_e} \end{bmatrix}. \quad (7)$$

Values of noisy response data  $e_{y,j}^{(t)}$  depend on the type of TR. For linear TR, we may set  $e_{y,j}^{(t)} \equiv 0$ , the sample mean  $\bar{y}$ , or any other constant  $d$  for  $j = 1, \dots, n_e$ ; for logistic TR with  $Y = \{0, 1\}$ , we may set half of  $n_e$   $e_{y,j}^{(t)}$ 's at 0 and the other half at 1; for Poisson and negative binomial TR, we may set  $e_{y,j}^{(t)} = 1$  for  $j = 1, \dots, n_e$ . Augmented tensor predictor  $\mathcal{Z}_j^{(t)}$  is constructed from the components of a Tucker decomposition; that is,

$$\begin{aligned} \mathcal{Z}_j^{(t)} &\triangleq \mathcal{E}_j^{(t)} \times_1 \mathbf{U}_1^{(t-1)} \times_2 \mathbf{U}_2^{(t-1)} \times_3 \dots \times_D \mathbf{U}_D^{(t-1)} \\ &= \sum_{r_1=1}^{R_1} \sum_{r_2=1}^{R_2} \dots \sum_{r_D=1}^{R_D} e_{j,i_1 i_2 \dots i_D}^{(t)} \mathbf{u}_1^{r_1(t-1)} \circ \mathbf{u}_2^{r_2(t-1)} \circ \dots \circ \mathbf{u}_D^{r_D(t-1)}, \end{aligned} \quad (8)$$

$$\text{where } e_{j,i_1 i_2 \dots i_D}^{(t)} \sim \mathcal{N}(0, \lambda (g_{r_1 r_2 \dots r_D}^{(t-1)})^{-2}), \quad (9)$$

$\lambda$  is a hyperparameter (tuned or prespecified),  $g_{r_1 r_2 \dots r_D}^{(t-1)}$  is the element  $[r_1, r_2, \dots, r_D]$  in the core tensor  $\mathcal{G}^{(t-1)}$ , and  $\mathbf{U}_i^{(t-1)}$  for  $i = 1, \dots, D$  is the estimate of  $\mathbf{U}_i$  from iteration  $t - 1$ ; both  $\mathcal{G}^{(t-1)}$  and  $\mathbf{U}_i^{(t-1)}$  are the components in the Tucker decomposition of estimate  $\mathcal{B}^{(t-1)}$ . Eq (9) is referred to as the *noise-generating distribution*, a Gaussian distribution with an adaptive variance term that is designed to achieve  $\ell_0$  regularization. In addition,  $n_e$  needs to be  $< p$ , where  $p$  is the total number of elements in  $\mathbf{G}$ , to achieve the  $\ell_0$  regularization (the number of zero elements in theory in  $\mathbf{G}$  is  $n_e$ ; established in Sections 3.1).

After the noisy data are generated, we run a regular GLM to obtain an updated estimate  $\mathcal{B}^{(t)}$  by minimizing the loss function formulated given the noise-augmented data, which is

$$\begin{aligned} l_{na}^{(t)} &= l(\mathcal{B}, \phi | \mathbf{y}_i, \mathcal{X}_i, e_{y,j}^{(t)}, \mathcal{Z}_j^{(t)}, 1 \leq i \leq n, 1 \leq j \leq n_e) \\ &= -\sum_{i=1}^n \ln p(y_i | \mathcal{X}_i, \mathcal{B}, \phi) - \sum_{j=1}^{n_e} \ln p(e_{y,j}^{(t)} | \mathcal{Z}_j^{(t)}, \mathcal{B}, \phi). \end{aligned} \quad (10)$$

This step can leverage any software that runs regular GLM (without regularization) without a need to design or code an optimization procedure to estimate  $\mathcal{B}$ .

In what follows, we establish theoretically that NA<sub>0</sub>CT<sup>2</sup> achieves  $\ell_0$  regularization on the core tensor  $\mathcal{G}$  upon convergence. We first examine linear TR with Gaussian  $Y$  (Section 3.1) and then extend the conclusion to GLM TR in general (Section 3.2).

### 3.1 $\ell_0$ regularization via NA<sub>0</sub>CT<sup>2</sup> in Linear TR

In linear TR, the loss function reduces to a  $\ell_2$  loss. Given observed data  $(\mathcal{X}_i, y_i)$  for  $i = 1, \dots, n$  and noisy data  $(\mathcal{Z}_i, e_{y,j} \equiv d)$  for  $j = 1, \dots, n_e$  that augment the former, the loss function is

$$\begin{aligned} l_{na} &= \sum_{i=1}^n (y_i - \langle \mathcal{X}_i, \mathcal{B} \rangle)^2 + \sum_{j=1}^{n_e} (e_{y,j} - \langle \mathcal{Z}_i, \mathcal{B} \rangle)^2 \\ &= \sum_{i=1}^n (y_i - \langle \mathcal{X}_i, \mathcal{B} \rangle)^2 + n_e d^2 - 2d \sum_{j=1}^{n_e} \langle \mathcal{Z}_j, \mathcal{B} \rangle + \sum_{j=1}^{n_e} \langle \mathcal{Z}_j, \mathcal{B} \rangle^2. \end{aligned} \quad (11)$$

Eq (11) contains both a linear term and a quadratic term in  $\mathcal{B}$ . We show below that it is the quadratic term that yields  $\ell_0$  regularization. Toward that end, augmented noisy data need to be designed in a way such that the linear term is zero so to avoid any undesirable regularization effect on  $\mathcal{B}$  from the linear term. In the linear TR case, there are two ways to achieve the goal. First, we can set  $e_{y,j} \equiv 0$  for all  $j = 1, \dots, n_e$ , in which case, the linear term  $2d \sum_{j=1}^{n_e} \langle \mathcal{Z}_j, \mathcal{B} \rangle = 0$  in Eq (11). Second, we generate two blocks of noisy terms, each

of size  $n_e$ . The first  $n_e$  terms contain noisy data points  $(e_{y,j}, \mathcal{Z}_j)$  for  $1 \leq j \leq n_e$  and the second block contains data points  $(e_{y,j} = e_{y,j-n_e}, \mathcal{Z}_j = -\mathcal{Z}_{j-n_e})$  for  $n_e + 1 \leq j \leq 2n_e$ , as demonstrated in Eq (12),

$$\begin{bmatrix} (\mathcal{X}_i, y_i)_{i=1,\dots,n} \\ (\mathcal{Z}_j^{(t)}, e_{y,j}^{(t)})_{j=1,\dots,2n_e} \end{bmatrix} = \begin{bmatrix} (\mathcal{X}_i, y_i)_{i=1,\dots,n} \\ (\mathcal{Z}_j^{(t)}, e_{y,j}^{(t)})_{j=1,\dots,n_e} \\ (-\mathcal{Z}_j^{(t)}, e_{y,j}^{(t)})_{j=1,\dots,n_e} \end{bmatrix}. \quad (12)$$

The linear term in Eq (11) also becomes 0 as  $\sum_{j=1}^{n_e} \langle \mathcal{Z}_j, \mathcal{B} \rangle + \sum_{j=n_e+1}^{2n_e} \langle \mathcal{Z}_j, \mathcal{B} \rangle = 0$  per the design in Eq (12). In summary, both noise augmentation schemes lead to

$$l_{na} = \sum_{i=1}^n (y_i - \langle \mathcal{X}_i, \mathcal{B} \rangle)^2 + C_1 \sum_{j=1}^{n_e} \langle \mathcal{Z}_j, \mathcal{B} \rangle^2 + C_2, \quad (13)$$

where  $C_1 = 1, C_2 = 0$  if we set  $e_{y,j} \equiv 0$  and  $C_1 = 2, C_2 = 2n_e d^2$  if we use the two-block noise augmentation scheme. We now show the quadratic term  $\sum_{j=1}^{n_e} \langle \mathcal{Z}_j, \mathcal{B} \rangle^2$  in Eq (13) leads to  $\ell_0$  regularization on the core tensor of  $\mathcal{B}$  if Tucker decomposition is applied to  $\mathcal{Z}$  and  $\mathcal{B}$ . The inner product  $\langle \mathcal{Z}_j, \mathcal{B} \rangle$  in Eq (13), after Tucker decomposition on  $\mathcal{B}$  and given how  $\mathcal{Z}$  is designed, can be written as

$$\begin{aligned} & \left\langle \sum_{i_1=1}^{R_1} \sum_{i_2=1}^{R_2} \dots \sum_{i_D=1}^{R_D} e_{j,i_1 i_2 \dots i_D} \mathbf{u}_1^{i_1} \circ \mathbf{u}_2^{i_2} \circ \dots \circ \mathbf{u}_D^{i_D}, \sum_{i_1=1}^{R_1} \sum_{i_2=1}^{R_2} \dots \sum_{i_D=1}^{R_D} g_{i_1 i_2 \dots i_D} \mathbf{u}_1^{i_1} \circ \mathbf{u}_2^{i_2} \circ \dots \circ \mathbf{u}_D^{i_D} \right\rangle \\ &= \sum_{i_1=1}^{R_1} \sum_{i_2=1}^{R_2} \dots \sum_{i_D=1}^{R_D} \langle e_{j,i_1 i_2 \dots i_D} \mathbf{u}_1^{i_1} \circ \mathbf{u}_2^{i_2} \circ \dots \circ \mathbf{u}_D^{i_D}, g_{i_1 i_2 \dots i_D} \mathbf{u}_1^{i_1} \circ \mathbf{u}_2^{i_2} \circ \dots \circ \mathbf{u}_D^{i_D} \rangle + \\ & \quad \sum_{i_d \neq j_d, 1 \leq i_d, j_d \leq R_d} \langle e_{j,i_1 i_2 \dots i_D} \mathbf{u}_1^{i_1} \circ \mathbf{u}_2^{i_2} \circ \dots \circ \mathbf{u}_D^{i_D}, g_{j_1 i_2 \dots j_D} \mathbf{u}_1^{j_1} \circ \mathbf{u}_2^{j_2} \circ \dots \circ \mathbf{u}_D^{j_D} \rangle \end{aligned} \quad (14)$$

$$= \sum_{i_1=1}^{R_1} \sum_{i_2=1}^{R_2} \dots \sum_{i_D=1}^{R_D} e_{j,i_1 i_2 \dots i_D} g_{i_1 i_2 \dots i_D}, \quad (15)$$

Eq (15) holds due to the orthonormality of the columns in  $\mathbf{u}_d$  (thus  $\langle \mathbf{u}_1^{i_1} \circ \mathbf{u}_2^{i_2} \circ \dots \circ \mathbf{u}_D^{i_D}, \mathbf{u}_1^{i_1} \circ$

$\mathbf{u}_2^{i_2} \circ \dots \circ \mathbf{u}_D^{i_D} \rangle = 1$  in the first term and the second term in Eq (14) is zero). Substituting  $\langle \mathcal{Z}_j, \mathcal{B} \rangle$  in Eq (13) with Eq (15), we have

$$l_{na} = \sum_{i=1}^n (y_i - \langle \mathcal{X}_i, \mathcal{B} \rangle)^2 + C_1 \sum_{j=1}^{n_e} \left( \sum_{i_1=1}^{R_1} \sum_{i_2=1}^{R_2} \dots \sum_{i_D=1}^{R_D} g_{i_1 i_2 \dots i_D} e_{j, i_1 i_2 \dots i_D} \right)^2 + C_2 \quad (16)$$

$$= \sum_{i=1}^n (y_i - \langle \mathcal{X}_i, \mathcal{B} \rangle)^2 + \lambda \sum_{j=1}^{n_e} \left( \sum_{i_1=1}^{R_1} \sum_{i_2=1}^{R_2} \dots \sum_{i_D=1}^{R_D} g_{i_1 i_2 \dots i_D} e'_{j, i_1 i_2 \dots i_D} \right)^2 + C_2, \quad (17)$$

$$\text{where } e'_{j, i_1 i_2 \dots i_D} = \lambda^{-1/2} e_{j, i_1 i_2 \dots i_D} \sim \mathcal{N}(0, g_{i_1 i_2 \dots i_D}^{-2}). \quad (18)$$

Eq (17) suggests that the second term of the loss function formulated on augmented noisy data serves as a regularization term on the core tensor  $\mathcal{G}$  of  $\mathcal{B}$ . In fact, the optimization problem in Eq (17) is the Lagrange expression of the constrained optimization in Eqn (19) when the same multiplier  $\lambda$  is used for all  $n_e$  constrained terms.

$$\begin{aligned} & \min_{\mathcal{B}} \sum_{i=1}^n (y_i - \langle \mathcal{X}_i, \mathcal{B} \rangle)^2 \\ & \text{subject to } \sum_{i_1=1}^{R_1} \sum_{i_2=1}^{R_2} \dots \sum_{i_D=1}^{R_D} g_{i_1 i_2 \dots i_D} e'_{1, i_1 i_2 \dots i_D} = 0 \\ & \quad \sum_{i_1=1}^{R_1} \sum_{i_2=1}^{R_2} \dots \sum_{i_D=1}^{R_D} g_{i_1 i_2 \dots i_D} e'_{2, i_1 i_2 \dots i_D} = 0, \\ & \quad \vdots \\ & \quad \sum_{i_1=1}^{R_1} \sum_{i_2=1}^{R_2} \dots \sum_{i_D=1}^{R_D} g_{i_1 i_2 \dots i_D} e'_{n_e, i_1 i_2 \dots i_D} = 0. \end{aligned} \quad (19)$$

We can also view the constraint in Eq (19) as promoting orthogonality between the core tensor elements  $g$ 's and augmented noisy tensor predictors. The smaller an element  $g$  is, the larger the variance of the noise-generating distribution, and the more dispersed the corresponding noisy predictor is and the less relevant it is in the TR model, further pushing the estimated value of  $g$  towards zero, until stabilization and convergence. Since the core tensor represents the interaction among the factor matrices in the Tucker decomposition of  $\mathcal{B}$ , it being sparse implies that there are only limited interactions among the factor matrices,

which helps with interpretations.

Proposition 1 states the constrained optimization Eqn (19) is  $\ell_0$  regularization with exactly  $n_e$  elements in  $\mathcal{G}$  set at 0. The proof is straightforward. There are  $n_e$  linear constraints on the elements  $g$ 's of in  $\mathcal{G}$  in Eqn (19), the coefficients of which are noise terms drawn independently from the noise-generating distribution, implying that exactly  $n_e$  entries can be expressed exactly as a linear function of the rest of the components in  $\mathcal{G}$ ; in other words,  $n_e$  components in the core tensor can be set at 0.

**Proposition 1** ( $\ell_0$  regularization on core tensor in linear TR through NA<sub>0</sub>CT<sup>2</sup>). The constrained optimization problem in Eqn (19) is equivalent to

$$\begin{aligned} & \min_{\mathcal{B}} \sum_{i=1}^n (y_i - \langle \mathcal{X}_i, \mathcal{B} \rangle)^2 \\ & \text{subject to } \sum_{i_1=1}^{R_1} \sum_{i_2=1}^{R_2} \cdots \sum_{i_D=1}^{R_D} \mathbb{1}(g_{i,i_1 i_2 \dots i_D} = 0) = n_e. \end{aligned} \quad (20)$$

Since  $g_{i,i_1 i_2 \dots i_D}$  is unknown, the iterative NA<sub>0</sub>CT<sup>2</sup> procedure would require users to supply an initial  $\mathcal{B}^{(0)}$  and then use the estimates of  $\mathcal{G}$  from the previous iteration when sampling noisy tensor predictor data in Eq (9). Upon convergence, the estimate of  $\mathcal{G}$  stabilizes, and so is the noise-generating distribution; but the random fluctuation in the estimate of  $\mathcal{G}$  still exists from iteration to iteration given that randomly sampled noisy data are different across the iterations. For that reason, while the  $\ell_0$  regularization via NA<sub>0</sub>CT<sup>2</sup> is exact conceptually, the realized regularization in actual implementations of NA<sub>0</sub>CT<sup>2</sup> would only get arbitrarily close to  $\ell_0$  due to the random fluctuation. One way to mitigate the numerical randomness around the estimate of  $\mathcal{B}$  so to get as close as possible to exact  $\ell_0$  is to take the average of estimated parameters over multiple iterations upon convergence; details are provided in Algorithm 1 of Section 3.3.

### 3.2 $\ell_0$ regularization via $\text{NA}_0\text{CT}^2$ in GLM TR

When  $Y$  follows an exponential family distribution in Eq (1), the loss function can be formulated as a negative log-likelihood. We employ the same noisy-data augmentation scheme as in Eq (12) with the two blocks of noisy data, each of size  $n_e$  with opposite signs on the noisy predictor tensor when augmenting the loss function for  $\text{NA}_0\text{CT}^2$ ; that is,

$$\begin{aligned} l_{na}(\mathcal{B}, \phi | y_i, \mathcal{X}_i, e_{y,j}, \mathcal{Z}_j, 1 \leq i \leq n, 1 \leq j \leq 2n_e) \\ = - \sum_{i=1}^n \ln p(y_i | \mathcal{X}_i, \mathcal{B}, \phi) - \sum_{j=1}^{n_e} \ln p(e_{y,j} | \mathcal{Z}_j, \mathcal{B}, \phi) - \sum_{j=n_e+1}^{2n_e} \ln p(e_{y,j} | -\mathcal{Z}_j, \mathcal{B}, \phi). \end{aligned} \quad (21)$$

**Proposition 2** ( $\ell_0$  regularization on core tensor in general TR through  $\text{NA}_0\text{CT}^2$ ). Minimization of the augment loss function in Eqn (21) is equivalent to

$$\begin{aligned} \min_{\mathcal{B}} - \sum_{i=1}^n \ln p(y_i | \mathcal{X}_i, \mathcal{B}, \phi) \\ \text{subject to } \sum_{i_1=1}^{R_1} \sum_{i_2=1}^{R_2} \cdots \sum_{i_D=1}^{R_D} \mathbb{1}(g_{i,i_1 i_2 \dots i_D} = 0) = n_e. \end{aligned} \quad (22)$$

Propositions 2 is proved as follows. Applying the Taylor expansion around  $\langle \mathcal{Z}_j, \mathcal{B} \rangle = 0$ ,  $l_{na}$  in Eq (21) becomes

$$\begin{aligned} & - \sum_{i=1}^n \ln p(y_i | \mathcal{X}_i, \mathcal{B}, \phi) - \sum_{j=1}^{n_e} \left\{ \frac{-B(0)}{a(\phi)} + h(e_{y,j}, \phi) + \frac{e_{y,j} - B'(0)}{a(\phi)} \langle \mathcal{Z}_j, \mathcal{B} \rangle + \frac{B''(0)}{2a(\phi)} \langle \mathcal{Z}_j, \mathcal{B} \rangle^2 \right. \\ & \left. + O(\langle \mathcal{Z}_j, \mathcal{B} \rangle^3) + O(\langle \mathcal{Z}_j, \mathcal{B} \rangle^4) + \dots \right\} - \sum_{j=n_e+1}^{2n_e} \left\{ \frac{-B(0)}{a(\phi)} + h(e_{y,j}, \phi) + \frac{e_{y,j} - B'(0)}{a(\phi)} \langle -\mathcal{Z}_j, \mathcal{B} \rangle \right. \\ & \left. + \frac{B''(0)}{2a(\phi)} \langle -\mathcal{Z}_j, \mathcal{B} \rangle^2 + O(\langle -\mathcal{Z}_j, \mathcal{B} \rangle^3) + O(\langle -\mathcal{Z}_j, \mathcal{B} \rangle^4) + \dots \right\} \\ & = - \sum_{i=1}^n \ln p(y_i | \mathcal{X}_i, \mathcal{B}, \phi) + C_1 \sum_{j=1}^{n_e} \sum_{l=1}^{\infty} \langle \mathcal{Z}_j, \mathcal{B} \rangle^{2l} + C_2, \end{aligned} \quad (23)$$

where  $C_1 = -B''(0)/(a(\phi))$  and  $C_2 = 2n_e B(0)/a(\phi) - \sum_{j=1}^{2n_e} h(e_{y,j}, \phi)$  are constant independent of  $\mathcal{B}$ . The augmented loss function in Eq (23) compared to the regularization term

in Eq (13) in linear TR, has additional even exponents of  $\langle \mathcal{Z}_j, \mathcal{B} \rangle$  in addition to the quadratic term  $\langle \mathcal{Z}_j, \mathcal{B} \rangle^{2l}$ . These additional even-powered terms of  $\langle \mathcal{Z}_j, \mathcal{B} \rangle$  have the same regularization effect as the quadratic term, which is orthogonality constraints between  $\mathbf{e}_j$  and the core tensor  $\mathcal{G}$  or the  $\ell_0$  regularization on  $\mathcal{G}$  just as in the case of linear TR. Therefore, the statements from Propositions 1 also apply to the GLM TR setting,

### 3.3 Algorithm for $\text{NA}_0\text{CT}^2$

Algorithm 1 lists the steps for running the  $\text{NA}_0\text{CT}^2$  procedure. The algorithm uses an explicitly specified stopping criterion. Besides that, plotting trace plots of loss functions to eyeball the convergence or examine the change in the estimate of  $\hat{\mathcal{B}}$  across iterations such as  $\|\bar{\mathcal{B}}^{(t)} - \bar{\mathcal{B}}^{(t-1)}\|_1 \leq \eta$ , where  $\eta$  is a small constant, can also be used to evaluate convergence.

Users need to supply an initial set of parameters, such as from the regression model on vectorized  $\mathcal{X}_i$ , which can be regularized or not, as given in line 2. The algorithm also includes a moving window  $m > 1$  to help to smooth out the randomness in the estimated tensor  $\hat{\mathcal{B}}$  and in the loss function since augmented noisy data change at every iteration. The usage of  $m$  is algorithmic and doesn't affect the theoretical property of  $\text{NA}_0\text{CT}^2$  established in Proposition 1. Since the variances of noise-generating Gaussian distributions are inversely proportional to the squared core tensor entry values, the estimates of zero-valued entries in the core tensor via  $\text{NA}_0\text{CT}^2$  would shrink toward 0 upon the convergence of the algorithm, leading to very large variances in the noise-generating distributions and potential overflows when running the algorithm. To avoid this, we recommend lower bounding the estimated elements in the core tensor by a very small constant  $\tau_0$  (e.g,  $10^{-10}$ ).

For the choice of hyper-parameter  $\lambda$ , the empirical studies we conducted indicate that the performance of  $\text{NA}_0\text{CT}^2$  is rather robust to a wide range of  $\lambda$  ( $\lambda = 5 \sim 500$  in Section 4). The value of  $n_e$  is more influential on the performance of  $\text{NA}_0\text{CT}^2$  and needs to be carefully chosen. Since  $n_e$  can be regarded as the number of zeroes in the core tensor, it should be

smaller than the components in the core tensor. On the other hand,  $n_e$  too small would result in a minimal regularization effect.  $n_e$  can be tuned through cross-validation (CV) and examining information criteria (e.g. AIC) from GLMs.

---

**Algorithm 1:** The NA<sub>0</sub>CT<sup>2</sup> procedure

---

**input :** observed data  $(\mathcal{X}_i, y_i)$  for  $i = 1, \dots, n$ ; noisy data size  $n_e$ , noisy response data  $e_{y,j}$  for  $j = 1, \dots, n_e$ ; regularization hyperparameter  $\lambda$ ; maximum iterations  $T$ ; stopping thresholds  $\tau$  or  $\eta$ ; zero threshold  $\tau_0$ , moving average window  $m$

**output:** TR coefficient tensor  $\hat{\mathcal{B}}$

- 1 Standardize  $\mathcal{X}_i$  for each  $1 \leq i \leq n$ ;
- 2 Calculate  $\hat{\mathcal{B}}$  from regression model on  $Y$  on vectorized  $\mathcal{X}_i$  and set  $\bar{\mathcal{B}}^{(0)} = \hat{\mathcal{B}}^{(0)} = \hat{\mathcal{B}}$ ;
- 3  $t \leftarrow 1$ , convergence status  $s \leftarrow 0$ ;
- 4 **while**  $t \leq T$  and  $s = 0$  **do**
  - 5 Apply Tucker decomposition to  $\hat{\mathcal{B}}^{(t-1)} = \hat{\mathcal{G}}^{(t-1)} \times_1 \hat{\mathbf{U}}_1^{(t-1)} \times_2 \hat{\mathbf{U}}_2^{(t-1)} \times_3 \cdots \times_D \hat{\mathbf{U}}_D^{(t-1)}$ ;
  - 6 **if**  $t \leq m$  **then**
    - 7  $\bar{\mathcal{G}}^{(t-1)} \leftarrow \hat{\mathcal{G}}^{(t-1)}$ ;
  - 8 **else**
    - 9  $\bar{\mathcal{G}}^{(t-1)} \leftarrow \{ \sum_{i=t-m-1}^t \hat{\mathcal{G}}^{(i)} / m + c \}$ ;  
//  $c$  is a small constant (e.g.,  $10^{-7}$ ) to avoid overflow of  $(\bar{\mathcal{G}}^{(t-1)})^{-2}$ .
  - 10 **end**
  - 11 Generate elements in the core tensor  $\mathcal{E}_j^{(t)}$  of the noisy predictor  $\mathcal{Z}_j$ :  
 $e_{j,i_1 i_2 \dots i_D} \sim N(0, \lambda (\bar{g}_{i_1 i_2 \dots i_D}^{(t-1)})^{-2})$  for  $j = 1, \dots, n_e$ ,  $i_d = 1, \dots, R_d$ , and  $d = 1, \dots, D$ ;
  - 12 Calculate  $\mathcal{Z}_j = \mathcal{E}_j^{(t)} \times_1 \hat{\mathbf{U}}_1^{(t-1)} \times_2 \hat{\mathbf{U}}_2^{(t-1)} \times_3 \cdots \times_D \hat{\mathbf{U}}_D^{(t-1)}$  for  $j = 1, \dots, n_e$ ;
  - 13 Combine  $(\mathcal{X}_i, y_i)_{i=1, \dots, n}$ ,  $(\mathcal{Z}_j^{(t)}, e_{y,j})_{j=1, \dots, n_e}$ , and  $(-\mathcal{Z}_j^{(t)}, e_{y,j})_{j=1, \dots, n_e}$  to form an augmented dataset of size  $n + 2n_e$ ;
  - 14 Run GLM on the augmented data with vectorized predictor  
 $\text{vec}(\mathcal{X}_i, \mathcal{Z}_j^{(t)})_{i=1, \dots, n; j=1, \dots, 2n_e}$  and response  $(y_i, e_{y,j})_{i=1, \dots, n; j=1, \dots, 2n_e}$  to obtain updated estimate  $\hat{\mathcal{B}}^{(t)}$ ;
  - 15 **if**  $t \leq m$  **then**
    - 16  $\bar{\mathcal{B}}^{(t)} \leftarrow \hat{\mathcal{B}}^{(t)}$  and  $\bar{l}^{(t)} \leftarrow \hat{l}(\hat{\mathcal{B}}^{(t)})$ ;
  - 17 **else**
    - 18  $\bar{\mathcal{B}}^{(t)} \leftarrow \sum_{i=t-m-1}^t \hat{\mathcal{B}}^{(i)} / m$  and  $\bar{l}^{(t)} \leftarrow \sum_{i=t-m-1}^t \hat{l}(\hat{\mathcal{B}}^{(i)}) / m$ ;
  - 19 **end**
  - 20 **if**  $|\bar{l}^{(t)} - \bar{l}^{(t-1)}| \leq \tau$  or  $\|\bar{\mathcal{B}}^{(t)} - \bar{\mathcal{B}}^{(t-1)}\|_1 \leq \eta$  **then**
    - 21  $s = 1$ ;
  - 22 **end**
  - 23  $t \leftarrow t + 1$ ;
- 24 **end**
- 25 Output  $\bar{\mathcal{B}}^{(t)}$ . // the next two steps are optional
- 26 Apply Tucker decomposition to  $\bar{\mathcal{B}}^{(t)}$  to obtain  $\hat{\mathcal{G}} \times_1 \hat{\mathbf{U}}_1 \times_2 \hat{\mathbf{U}}_2 \times_3 \cdots \times_D \hat{\mathbf{U}}_D$ , replace any element in  $\hat{\mathcal{G}}$  that is  $\leq \tau_0$  with 0 to obtain a new  $\mathcal{G}_0$ ;
- 27 Output  $\hat{\mathcal{B}} = \hat{\mathcal{G}}_0 \times_1 \hat{\mathbf{U}}_1 \times_2 \hat{\mathbf{U}}_2 \times_3 \cdots \times_D \hat{\mathbf{U}}_D$ .

---



## 4 Numerical Examples

We apply  $\text{NA}_0\text{CT}^2$  in four numerical examples. The first three examples use simulated data on three different types of responses (Gaussian, binary, count), and the last example is on a real image dataset with continuous responses. We compare  $\text{NA}_0\text{CT}^2$  with the following competing regression approaches in outcome prediction in all examples and also examine the ability of feature selection in the real data example.

- GLM on vectorized predictors  $\text{vec}(\mathcal{X})$ , unregularized and with  $\ell_1$  regularization.
- TR with CP decomposition on  $\mathcal{B}$ , unregularized and with  $\ell_2$  regularization on the entries  $\mathbf{U}_d$  for  $d = 1, 2, \dots, D$  of  $\mathcal{B}$  after decomposed (Eq (3)) (Zhou et al., 2013).
- TR with Tucker decomposition on  $\mathcal{B}$ , unregularized and with  $\ell_1$  regularization on the core tensor (Li et al., 2018).
- $\text{NA}_0\text{CT}^2$  : TR with Tucker decomposition on  $\mathcal{B}$  with  $\ell_0$ -regularization on the core tensor (our method).

To make the TR models based on Tucker decomposition and CP decomposition comparable, we set the numbers of free parameters roughly the same in these two types of TR models. We first set the dimensionality of the core tensor in the Tucker decomposition and calculated the total number of parameters according to Table 1. We then back-calculated the dimensionality  $R$  in the CP decomposition that yields the same or a similar number of parameters as with Tucker decomposition. The numbers of parameters in each model are listed in Table 2 for the 4 examples. Though the number of parameters in the Tucker and CP decomposition-based TR in the 3 simulation studies are the same as the GLM on  $\text{vec}(\mathcal{X})$ , the former two explore and leverage the structural information in tensor data and are expected to provide better prediction results.

Table 2: Number parameters of different methods in the examples

study	Tucker	CP	GLM on $\text{vec}(\mathcal{X})$
3 simulation studies	64	60	64
	$(R_1 = R_2 = R_3 = 4)$	$(R = 6)$	$(I_1 = I_2 = I_3 = 4)$
FG-NET	825	825	841
	$(R_1 = R_2 = 25)$	$(R = 25)$	$(I_1 = I_2 = 29)$
The dimensions $R_1$ and $R_2$ in the Tucker decomposition in the FG-NET applications were chosen by cross-validation.			

## 4.1 Simulation Studies

We examine three response types  $Y$  in the simulation studies – Gaussian, binary, and count; and run linear, logistic, and Poisson TR, respectively, each case given a tensor predictor  $\mathcal{X}$ . Respond data  $\mathbf{y}$  were generated from  $\mathcal{N}(\langle \mathcal{X}, \mathcal{B} \rangle, 0.5^2)$  and data on  $\mathcal{X}$  were generated from  $\mathcal{N}(0, 1)$  in the linear TR case,  $Y \sim \text{Bern}((1 + e^{-\langle \mathcal{B}, \mathcal{X} \rangle})^{-1})$  and data on  $\mathcal{X}$  were generated from  $\mathcal{N}(0, 0.25^2)$  in the logistic TR case, and  $Y \sim \text{Poisson}(e^{\langle \mathcal{B}, \mathcal{X} \rangle})$  and  $\mathcal{X}$  were generated from  $-2|\mathcal{N}(0.1, 0.3^2)| + 0.6$  in the Poisson case. Both  $\mathcal{B}$  and  $\mathcal{X}$  are of dimension  $4 \times 4 \times 4$ . Elements in  $\mathcal{B}$  were randomly generated from a certain distribution and were then adjusted to result in a sparse core tensor in the Tucker decomposition. Specifically, in the linear and logistic case, 8 elements of  $\mathcal{B}$  were first generated from  $\mathcal{N}(0, 1)$ , then were copied 8 times to formulate  $\mathcal{B}$ .  $\mathcal{B}$  in the Poisson case was constructed in a similar manner as in the logistic case, the only difference is that the initial 8 elements of  $\mathcal{B}$  were generated from  $\text{unif}(0, 0.3)$ . In all regression cases, the way in which  $\mathcal{B}$  is constructed results in 2 non-zero elements in the core tensor and 62 zero elements after Tucker decomposition. The sample size  $n$  of each training dataset was set at  $n = 300$  for the linear case,  $n = 300$  for the binary case, and  $n = 200$  for the Poisson case. The size of each testing dataset was set to 200.

For  $\text{NA}_0\text{CT}^2$ , we set  $n_e = 62$ ,  $\lambda = 50$ ,  $T = 30000$ ,  $m = 600$ ,  $\tau_0 = 10^{-6}$ ,  $\tau = 0.01$  in the linear TR;  $n_e = 62$ ,  $\lambda = 50$ ,  $T = 5000$ ,  $m = 600$ ,  $\tau_0 = 10^{-6}$ ,  $\tau = 0.01$  in the logistic TR; and  $n_e = 62$ ,  $\lambda = 50$ ,  $T = 10000$ ,  $m = 600$ ,  $\tau_0 = 10^{-6}$ ,  $\tau = 0.01$  in the Poisson TR. The TR models based on Tucker decomposition (Li et al., 2018) use an iterative block relaxation algorithm to estimate the parameters (Algorithm 2). Estimation of each “block”

of parameters given the rest parameters in each iteration is equivalent to running a GLM. The loss function  $l$  on lines 5 and 7 are log-likelihood functions. Two different TR models were run – with and without  $\ell_1$  regularization when estimating the core tensor. R package `glmnet` was used to run Algorithm 2. The hyperparameter for the  $\ell_1$  regularization was set at  $10^{-3}$  in the Poisson TR model (`cv.glmnet` resulted in errors) and was chosen by 5-fold cross-validation (CV) in the other cases.

---

**Algorithm 2:** TR based on Tucker decomposition (Li et al., 2018)

---

**input** : data  $(\mathcal{X}_i, y_i)$  for  $i = 1, \dots, n$ ; iterations  $T$ ; stopping threshold  $\eta$   
**output:** estimated coefficient tensor  $\hat{\mathcal{B}}$

- 1 Initialize  $\hat{\mathcal{G}}^{(0)} \in \mathbb{R}^{R_1 \times R_2 \times \dots \times R_D}$  and  $\hat{\mathbf{U}}_d^{(0)} \in \mathbb{R}^{I_d \times R_d}$  for  $d = 1, 2, \dots, D$ ;
- 2  $t \leftarrow 1$ , convergence status  $s \leftarrow 0$ ;
- 3 **while**  $t \leq T$  **and**  $s = 0$  **do**
- 4     **for**  $d = 1$  **to**  $D$  **do**
- 5          $\hat{\mathbf{U}}_d^{(t)} = \operatorname{argmax}_{\mathbf{U}_d} \sum_{i=1}^n l(\hat{\mathcal{G}}^{(t-1)}, \hat{\mathbf{U}}_1^{(t)}, \dots, \hat{\mathbf{U}}_{d-1}^{(t)}, \mathbf{U}_d, \hat{\mathbf{U}}_{d+1}^{(t-1)}, \dots, \hat{\mathbf{U}}_D^{(t-1)} | y_i, \mathcal{X}_i);$   
        // regularization when estimating of  $\mathbf{U}_d$  can be used.
- 6     **end**
- 7      $\hat{\mathcal{G}}^{(t)} = \operatorname{argmax}_{\mathcal{G}} \sum_{i=1}^n l(\mathcal{G}, \hat{\mathbf{U}}_1^{(t)}, \hat{\mathbf{U}}_2^{(t)}, \dots, \hat{\mathbf{U}}_D^{(t)} | y_i, \mathcal{X}_i);$   
        // regularization when estimating  $\mathcal{G}$  can be used.
- 8      $\hat{\mathcal{B}}^{(t)} = \hat{\mathcal{G}}^{(t)} \times_1 \hat{\mathbf{U}}_1^{(t)} \times_2 \hat{\mathbf{U}}_2^{(t)} \times_3 \dots \times_D \hat{\mathbf{U}}_D^{(t)};$
- 9     **if**  $\|\hat{\mathcal{B}}^{(t)} - \hat{\mathcal{B}}^{(t-1)}\|_1 \leq \eta$  **then**
- 10          $s = 1$ ;
- 11     **end**
- 12      $t \leftarrow t + 1$ ;
- 13 **end**
- 14 Output  $\hat{\mathcal{B}}^{(t)}$ .

---

The TR models based on the CP decomposition (Zhou et al., 2013) used the same iterative block relaxation algorithm to estimate the parameters (Algorithm 3). Two different TR models were run – with and without the  $\ell_2$  regularization when estimating  $\mathbf{U}_d$  for  $d = 1, 2, \dots, D$  in Eq (3). The hyperparameter for the  $\ell_2$  regularization was chosen by 5-fold CV

in each TR model case.

---

**Algorithm 3:** TR based on CP decomposition (Zhou et al., 2013)

---

**input :** data  $(\mathcal{X}_i, y_i)$  for  $i = 1, \dots, n$ ; maximum iterations  $T$ ; stopping threshold  $\eta$   
**output:** estimated coefficient tensor  $\hat{\mathcal{B}}$

- 1 Initialize  $\hat{\mathbf{U}}_d^{(0)} \in \mathbb{R}^{I_d \times R}$  for  $d = 1, 2, \dots, D$ ;
- 2  $t \leftarrow 1$ , convergence status  $s \leftarrow 0$ ;
- 3 **while**  $t \leq T$  and  $s = 0$  **do**
- 4      $d \leftarrow 1$ ;
- 5     **for**  $d = 1$  to  $D$  **do**
- 6          $\hat{\mathbf{U}}_d^{(t)} = \operatorname{argmax}_{\mathbf{U}_d} \sum_{i=1}^n l(\hat{\mathbf{U}}_1^{(t)}, \dots, \hat{\mathbf{U}}_{d-1}^{(t)}, \mathbf{U}_d, \hat{\mathbf{U}}_{d+1}^{(t-1)}, \dots, \hat{\mathbf{U}}_D^{(t-1)} | y_i, \mathcal{X}_i);$   
        // regularization when estimating  $\mathbf{U}_d$  can be used.
- 7     **end**
- 8      $\hat{\mathcal{B}}^{(t)} = \sum_{r=1}^R \hat{\mathbf{u}}_1^{(t),r} \circ \hat{\mathbf{u}}_2^{(t),r} \circ \dots \circ \hat{\mathbf{u}}_D^{(t),r}$  where  $\hat{\mathbf{u}}_d^{(t),r}$  is  $r^{\text{th}}$  column of  $\hat{\mathbf{U}}_d^{(t)}$ ;
- 9     **if**  $\|\hat{\mathcal{B}}^{(t)} - \hat{\mathcal{B}}^{(t-1)}\|_1 \leq \eta$  **then**
- 10          $s = 1$ ;
- 11     **end**
- 12      $t \leftarrow t + 1$ ;
- 13 **end**
- 14 Output  $\hat{\mathcal{B}}^{(t)}$ .

---

We run 200 repeats in each response type case and evaluated the prediction accuracy of the estimated TR models in the testing data, the accuracy of estimated or reconstructed  $\hat{\mathcal{B}}$ , and the accuracy in identifying zero and non-zero elements in the core tensor after the Tucker decomposition of  $\hat{\mathcal{B}}$ . When identifying zero and non-zero elements in the core tensor for TR models not based on Tucker decomposition, Tucker decomposition was applied to obtain a core tensor in each case. We then set  $\tau_0$  (the threshold for zero elements in the estimate core tensor) at 0.005, 0.05, and 0.05 for the linear, logistic, and Poisson TR, respectively.

The results are summarized in Table 3. In summary, NA<sub>0</sub>CT<sup>2</sup> has the smallest mean prediction error and MSE of  $\mathcal{B}$  compared to other regression methods in all three data types. In terms of the sparsity of the core tensor, NA<sub>0</sub>CT<sup>2</sup> is the only method that can effectively promote sparsity. While Tucker-decomposition-based TR with  $\ell_1$  regularized on the core tensor also promotes core tensor sparsity but it is far from enough given there are 62 0's in the core tensor in each regression case; in addition, it runs into numerical issues during the iterative optimization (during the iterations of the block relaxation algorithm in Algorithm

Table 3: Performance comparison among TR models in 3 simulation studies (200 repeats)

regression method	mean prediction error* (SD)	MSE <sup>#</sup> of $\mathcal{B}$	average number of 0 in core tensor
linear TR			
NA <sub>0</sub> CT <sup>2</sup>	<b>0.4114</b> (0.0181)	<b>0.0002</b>	<b>62.00</b>
unregularized Tucker	0.4487 (0.0213)	0.0011	17.50
$\ell_1$ regularized Tucker	0.4393 (0.0211)	0.0008	28.64
unregularized CP	0.4415 (0.0205)	0.0009	23.22
$\ell_2$ regularized CP	0.4269 (0.0203)	0.0006	26.06
vectorized	0.4487 (0.0213)	0.0011	17.50
$\ell_1$ regularized vectorized	0.4490 (0.0214)	0.0011	17.46
Poisson TR			
NA <sub>0</sub> CT <sup>2</sup>	<b>1.5639</b> (0.1110)	<b>0.0051</b>	<b>62.00</b>
unregularized Tucker	1.8391 (0.1626)	0.0165	25.22
$\ell_1$ regularized Tucker <sup>§</sup>	1.8272 (0.1625)	0.0160	25.90
unregularized CP	1.8154 (0.1593)	0.0156	27.20
$\ell_2$ regularized CP	1.6196 (0.1207)	0.0074	42.52
vectorized MLE	1.8391 (0.1626)	0.0165	25.23
$\ell_1$ regularized MLE	1.7307 (0.1216)	0.0136	28.35
logistic TR			
NA <sub>0</sub> CT <sup>2</sup>	<b>28.67%</b> (0.0246)	<b>0.1055</b>	<b>62.00</b>
unregularized Tucker	29.86% (0.0288)	0.8672	3.98
$\ell_1$ regularized Tucker	30.18% (0.0357)	0.6872	16.62
unregularized CP	29.85% (0.0207)	0.7542	3.00
$\ell_2$ regularized CP	29.18% (0.0259)	0.2378	13.26
vectorized	29.86% (0.0288)	0.8672	3.98
$\ell_1$ regularized vectorized	33.19% (0.0089)	0.3014	7.99
SVM	33.84% (0.0024)	-	-
<b>Bold numbers</b> represent the best performer by each metric in each TR model case.			
* averaged $\ell_1$ prediction error $(200n)^{-1} \sum_{j=1}^{200} \sum_{i=1}^n  \hat{y}_{ij} - y_i $ in testing data for linear and Poisson TR, where $\hat{y}_{ij}$ is the prediction for observation $i$ in repeat $j$ ; averaged misclassification rate over 200 repeats in testing data for logistic TR ( $\hat{y}_{ij} = 1$ if $\hat{\text{Pr}}(y_{ij} = 1) > 0.5$ , where $\hat{\text{Pr}}(y_{ij} = 1)$ is for observation $i$ in repeat $j$ , $\hat{y}_{ij} = 0$ otherwise.)			
<sup>#</sup> mean squared error $\sum_{i=1}^4 \sum_{j=1}^4 \sum_{k=1}^4 (\hat{b}_{ijk} - b_{ijk})^2 / 4^3$ , where $b_{ijk}$ is the true value of element $(i, j, k)$ in $\mathcal{B}$ , and $\hat{b}_{ijk}$ is its estimate averaged over 200 repeats.			
<sup>§</sup> The $\ell_1$ regularized Poisson TR model with Tucker decomposition had convergence problems. The metrics were calculated using 180 out of 200 repeats that converged.			

2, parameters are updated “blockwise” sequentially in the GLM framework with predictors  $\text{vec}(\mathcal{X})$  rescaled by the rest of the parameters. With an  $\ell_1$  regularized core tensor, some of the columns in the rescaled  $\text{vec}(\mathcal{X})$  contain only 0’s, resulting in a design matrix not of full rank with “redundant” features).

## 4.2 Real Data Application

We examined the performances of different TR methods in the FG-NET dataset (Fu et al., 2014) ([http://yanweifu.github.io/FG\\_NET\\_data/FGNET.zip](http://yanweifu.github.io/FG_NET_data/FGNET.zip)). It contains 1,002 human face images (color or greyscale) from 82 individuals aged from 0 to 69 years old. Each image is labeled with the person’s age and contains 68 manually annotated points, which describe the structure of a face and are located around the eyebrows, mouth, eyes, nose, and the edge of a face. We run linear TR with  $l_2$  loss to predict age given an image and identify pixels that are important predictors of age.

We first pre-processed the images before the model fitting. Specifically, we transformed all images to grayscale and used annotated points for a piecewise affine transformation that aligned the points and corners across all images. For example, the tip of the nose is located in the same position in a 2D Cartesian coordinate (xy) after transformation in each image; the same for all other points. We then stacked all transformed images to form a 3D block along the z-axis. The pre-processing procedure is illustrated with 3 examples in Figure 1.

We trained linear TR models on the final pre-processed gray-scaled  $29 \times 29$  images to predict age and to identify pixels that are important for age prediction (800 images were used as the training set, 100 images as the validation set, and the rest as the testing set).

For the  $\text{NA}_0\text{CT}^2$  procedure, we set  $n_e = 615$ ,  $\lambda = 50$ ,  $T = 10000$ ,  $m = 600$ ,  $\tau_0 = 10^{-6}$ , and  $\tau = 0.01$ . We used the validation set to select hyperparameters  $n_e$  and core tensor dimensions  $R_1$  and  $R_2$  (Table 2) for  $\text{NA}_0\text{CT}^2$  ( $\text{NA}_0\text{CT}^2$  is relatively robust to a wide range of  $\lambda$ ; in the two real data examples,  $\lambda$  from 50 to 500 yield similar results). For other TR models that involve regularization, we merged the training and validation set and used a five-fold CV to choose the hyperparameters. For TR models without regularization, we merge the training and validation set for training.

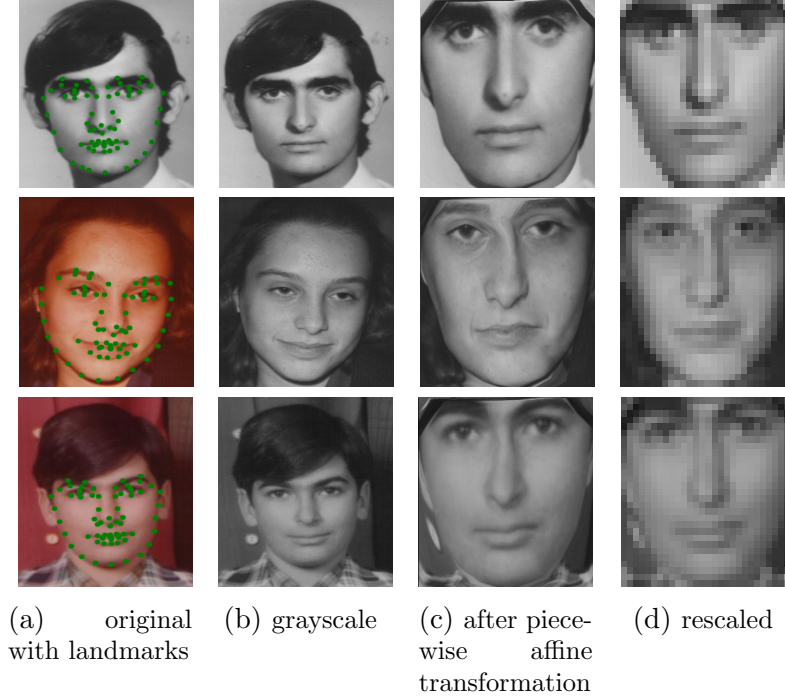


Figure 1: Pre-processing of the FG-NET images

We calculated the mean absolute prediction error  $\sum_{i=1}^n |\hat{y}_i - y_i|/n$  in both real applications, where  $n$  is the number of images in the testing data,  $y_i$  is the observed response, and  $\hat{y}_i$  is predicted response from each of the fitted TR models. The results are presented in Table 4.  $\text{NA}_0\text{CT}^2$  yields the smallest prediction error with a mean error 3.63 years, followed by the  $\ell_1$  regularized GLM on vectorized  $\mathcal{X}$  and  $\mathcal{B}$ , whereas the prediction errors in other TR models, regularized or not, are almost doubled or even quintupled.

Table 4: Predicted errors in different models in two real applications

$\text{NA}_0\text{CT}^2$	$\ell_1$ regularized GLM on $\text{vec}(\mathcal{X})$	$\ell_1$ -regularized Tucker	$\ell_2$ -regularized CP	unregularized CP	unregularized Tucker	GLM on $\text{vec}(\mathcal{X})$
<b>3.63</b>	4.30	7.11	9.51	20.57	20.57	20.80

We also examined the ability of TR models on their ability to identify important pixels in age prediction based on the estimated  $\hat{\mathcal{B}}$ . Note that among all the TR models used, only the  $\ell_1$ -regularized GLM sets some of the elements in estimated  $\hat{\mathcal{B}}$  at 0. Though the TR model based on the Tucker decompositions uses  $\ell_1$  regularization and  $\text{NA}_0\text{CT}^2$  achieves  $\ell_0$  regularization, the sparsity regularizations are imposed on the core tensor after Tucker decomposition of

$\mathcal{B}$  rather than  $\hat{\mathcal{B}}$  itself, and the sparsity of the core tensor does not necessarily translate into sparsity of  $\hat{\mathcal{B}}$ , which is constructed from the sparse core tensor and factor matrices  $\mathbf{U}$ 's. Figure 2 depicts the histograms of the elements in estimated  $\hat{\mathcal{B}}$  in each TR model. The magnitude of the elements in  $\hat{\mathcal{B}}$  varies significantly across different methods. The estimated elements from  $\text{NA}_0\text{CT}^2$  and  $\ell_1$ -regularized GLM are more similar in magnitude (ranging from around  $-1$  to  $1$  in the former and  $-4$  to  $3$  in the latter) while the other methods can produce extremely large values in  $\hat{\mathcal{B}}$  (e.g,  $\pm 70$ ).

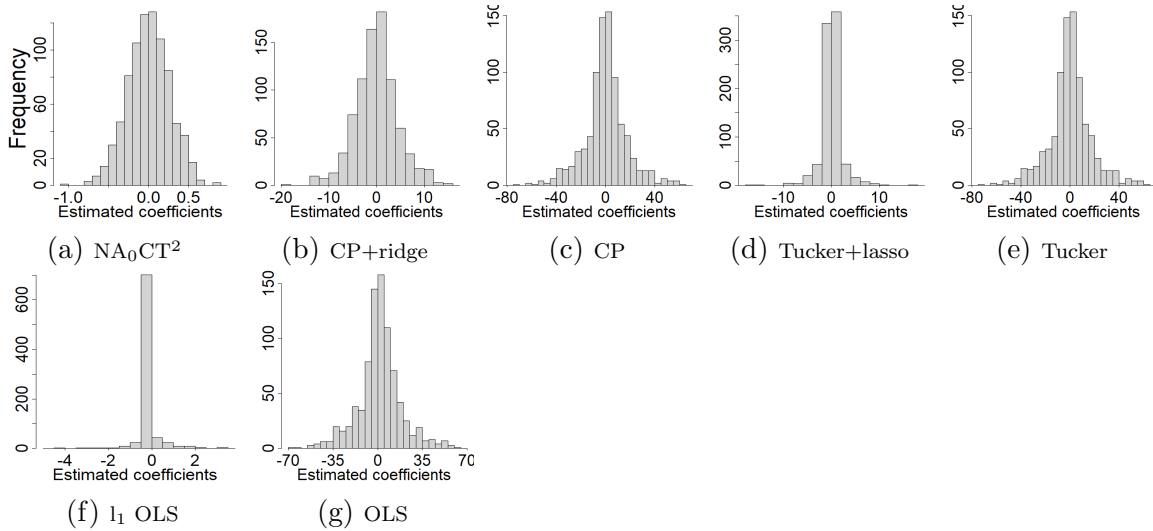
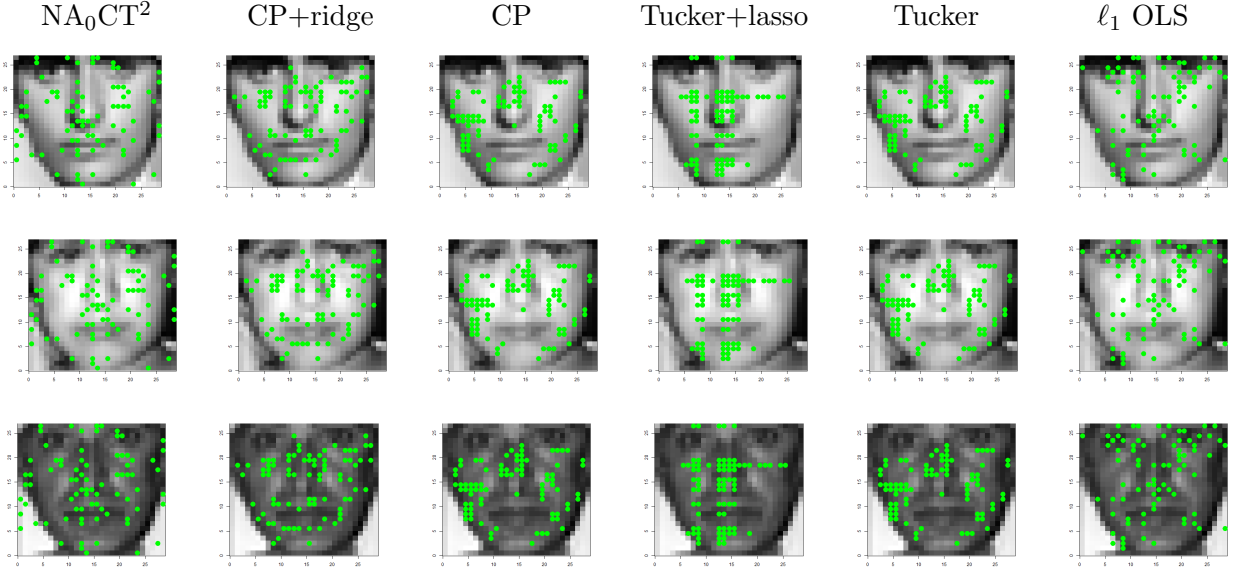


Figure 2: Histograms of estimated coefficients in different methods

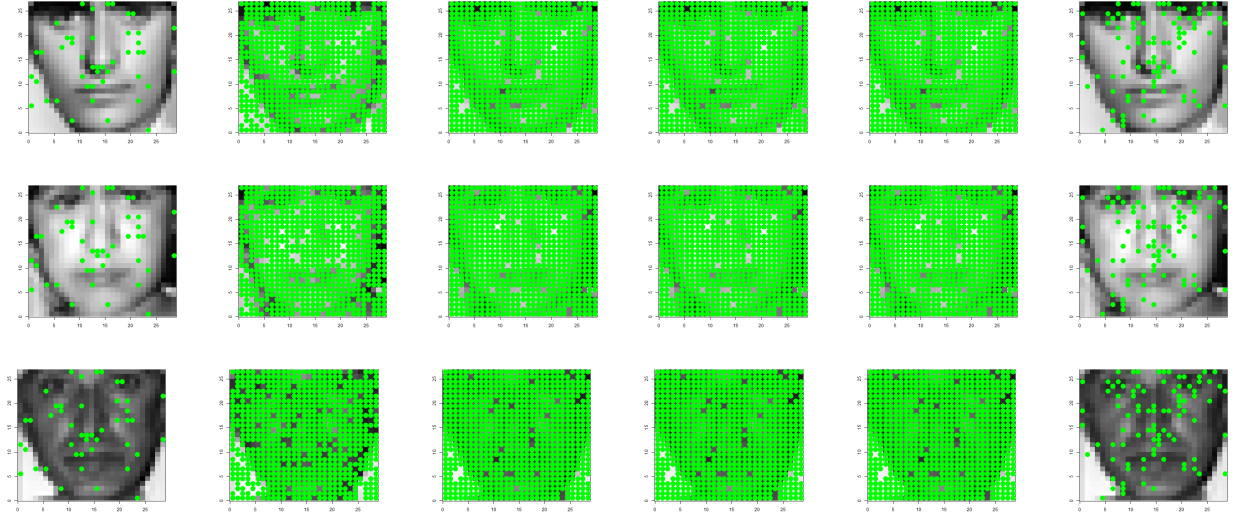
We took the top 10% elements in  $\hat{\mathcal{B}}$  in absolute value in each of the regression methods and plotted the corresponding pixels in Figure 3(a). We also applied hard thresholding at 0.5 to the absolute values of the elements in  $\hat{\mathcal{B}}$  and plotted the pixels with corresponding elements in  $|\hat{\mathcal{B}}| > 0.5$  in Figure 3(b). In both cases, the sparsity regularization imposed by  $\text{NA}_0\text{CT}^2$  on the core tensor, though not on  $\mathbf{B}$  directly, helps to locate pixels important for age prediction, which are concentrated around eyebrows, eyes, the area under the eyes, cheekbones, laugh lines, and the area around the mouth, and jawlines, which are all related to the early signs of aging (<https://www.skinmd.ph/blog-content/2017/12/8/the-anatomy-of-an-aging-face>). The  $\ell_1$  regularized linear regression with vectorized pre-



dictors also identifies similar important pixels for age predictions, many of which overlap those identified by  $\text{NA}_0\text{CT}^2$  but are more sparse. By contrast, the other TR models, regularized or not, select pixels that are not quite meaningful in terms of age prediction in Figure 3(a), or select overwhelmingly too many pixels in the hard-thresholding approach and do not help identify the important signs for age prediction.



(a) pixels corresponding to the top 10% elements in  $|\hat{\mathcal{B}}|$  are plotted



(b) pixels corresponding to elements in  $|\hat{\mathcal{B}}| > 0.5$  are plotted

Figure 3: Relevant pixels (green dots) for age prediction by different methods identified by two hard thresholding methods

## 5 Discussion

We propose  $\text{NA}_0\text{CT}^2$ , a regularization method for TR through noise augmentation, coupled with low-rank decomposition on the parameter tensor  $\mathcal{B}$ . We establish theoretically that  $\text{NA}_0\text{CT}^2$  promotes orthogonality between the core tensor and augmented noisy data and achieves exact  $\ell_0$  regularization in linear and GLM TR on the core tensor in the Tucker decomposition of  $\mathcal{B}$ . To our knowledge, our method is the first Tucker decomposition-based regularization method in TR to achieve  $\ell_0$  in core tensors.

$\text{NA}_0\text{CT}^2$  is implemented through an iterative procedure. Each iteration involves two simple steps – generating noisy data based on the core tensor estimates from the Tucker decomposition of the  $\mathcal{B}$  from the last iteration and running a regular GLM on noise-augmented data with vectorized predictors. Parameter estimates from  $\text{NA}_0\text{CT}^2$  are robust to the choice of hyperparameter  $\lambda$  while  $n_e$  requires careful tuning.  $\text{NA}_0\text{CT}^2$  outperforms other decomposition-based regularization methods for TR in both simulated data and real-life data applications and can also identify important predictors though it is not designed for that purpose.

For future work, we plan to apply  $\text{NA}_0\text{CT}^2$  to more complex tensor datasets, such as medical imaging data, to further explore the benefits of applying low-rank decomposition and the  $\ell_0$  regularization on the core tensor to TR in general and establish the asymptotic distributions of the estimated core tensor and estimated  $\mathcal{B}$  via the  $\text{NA}_0\text{CT}^2$  procedure, based on which confidential intervals of the parameters can be constructed. In addition, it would be of interest to quantify the convergence rate of the  $\text{NA}_0\text{CT}^2$  procedure in  $n$ , the number of parameters in  $\mathcal{B}$ , and the number of zero elements in the core tensor, and the fluctuations around the final estimates of the estimated parameters upon convergence.

The code for the  $\text{NA}_0\text{CT}^2$  procedure, the simulation study, and the real data applications is available at <https://github.com/AlvaYan/NA-L0-TR>.

## References

- Stephen Boyd, Neal Parikh, Eric Chu, Borja Peleato, Jonathan Eckstein, et al. Distributed optimization and statistical learning via the alternating direction method of multipliers. *Foundations and Trends® in Machine learning*, 3(1):1–122, 2011.
- J Douglas Carroll and Jih-Jie Chang. Analysis of individual differences in multidimensional scaling via an n-way generalization of “eckart-young” decomposition. *Psychometrika*, 35(3):283–319, 1970.
- Han Chen, Garvesh Raskutti, and Ming Yuan. Non-convex projected gradient descent for generalized low-rank tensor regression. *The Journal of Machine Learning Research*, 20(1):172–208, 2019.
- Ko-shin Chen, Tingyang Xu, Guannan Liang, Qianqian Tong, Minghu Song, and Jinbo Bi. An effective tensor regression with latent sparse regularization. *Journal of Data Science*, 20(2), 2022.
- Lee Dicker, Baosheng Huang, and Xihong Lin. Variable selection and estimation with the seamless- $l_0$  penalty. *Statistica Sinica*, 23:929–962, 2013.
- Yanwei Fu, Timothy M. Hospedales, Tao Xiang, Yuan Yao, and Shaogang Gong. Interest-iness prediction by robust learning to rank. In *ECCV*, 2014.
- Weiwei Guo, Irene Kotsia, and Ioannis Patras. Tensor learning for regression. *IEEE Transactions on Image Processing*, 21(2):816–827, 2011.
- Richard A Harshman et al. Foundations of the parafac procedure: Models and conditions for an” explanatory” multimodal factor analysis. *Working paper*, 1970.
- Lifang He, Kun Chen, Wanwan Xu, Jiayu Zhou, and Fei Wang. Boosted sparse and low-rank tensor regression. In *Advances in Neural Information Processing Systems*, pages 1009–1018, 2018.
- Mashud Hyder and Kaushik Mahata. An approximate  $l_0$  norm minimization algorithm for compressed sensing. In *2009 IEEE International Conference on Acoustics, Speech and Signal Processing*, pages 3365–3368. IEEE, 2009.
- Xiaoshan Li, Da Xu, Hua Zhou, and Lexin Li. Tucker tensor regression and neuroimaging analysis. *Statistics in Biosciences*, 10(3):520–545, 2018.
- Yinan Li and Fang Liu. Adaptive noisy data augmentation for regularized estimation and inference of generalized linear models. In *2022 IEEE 46th Annual Computers, Software, and Applications Conference (COMPSAC)*, pages 311–320, 2022. doi: 10.1109/COMPSAC54236.2022.00051.
- Yinan Li, Fang Liu, and Xiao Liu. Adaptive noisy data augmentation for regularized construction of undirected graphical models. In *2021 IEEE 8th International Conference on Data Science and Advanced Analytics (DSAA)*, pages 1–10. IEEE, 2021.

- Yuanyuan Liu, Fanhua Shang, Licheng Jiao, James Cheng, and Hong Cheng. Trace norm regularized candecomp/parafac decomposition with missing data. *IEEE transactions on cybernetics*, 45(11):2437–2448, 2014.
- Zhenqiu Liu and Gang Li. Efficient regularized regression with  $l_0$  penalty for variable selection and network construction. *Computational and Mathematical Methods in Medicine*, 3456153, 2016.
- Jinchi Lv and Yingying Fan. A unified approach to model selection and sparse recovery using regularized least squares. *The Annals of Statistics*, 37(6A):3498–3528, 2009.
- Le Ou-Yang, Xiao-Fei Zhang, and Hong Yan. Sparse regularized low-rank tensor regression with applications in genomic data analysis. *Pattern Recognition*, 107:107516, 2020.
- Garvesh Raskutti, Ming Yuan, Han Chen, et al. Convex regularization for high-dimensional multiresponse tensor regression. *The Annals of Statistics*, 47(3):1554–1584, 2019.
- Samrat Roy and George Michailidis. Regularized high dimension low tubal-rank tensor regression. *Electronic Journal of Statistics*, 16(1):2683–2723, 2022.
- Yueyong Shi, Yuanshan Wu, Deyi Xu, and Yuling Jiao. An admm with continuation algorithm for non-convex sica-penalized regression in high dimensions. *Journal of Statistical Computation and Simulation*, 88(9):1826–1846, 2018.
- Marco Signoretto, Quoc Tran Dinh, Lieven De Lathauwer, and Johan AK Suykens. Learning with tensors: a framework based on convex optimization and spectral regularization. *Machine Learning*, 94(3):303–351, 2014.
- Xiaonan Song and Haiping Lu. Multilinear regression for embedded feature selection with application to fmri analysis. In *Thirty-First AAAI Conference on Artificial Intelligence*, 2017.
- Wei Tang, Zhenwei Shi, and Zhana Duren. Sparse hyperspectral unmixing using an approximate  $l_0$  norm. *Optik*, 125(1):31–38, 2014.
- Ledyard R Tucker. Some mathematical notes on three-mode factor analysis. *Psychometrika*, 31(3):279–311, 1966.
- Sara van de Geer. Weakly decomposable regularization penalties and structured sparsity. *Scandinavian Journal of Statistics*, 41(1):72–86, 2014.
- Ziran Wei, Jianlin Zhang, Zhiyong Xu, Yongmei Huang, Yong Liu, and Xiangsuo Fan. Gradient projection with approximate  $\ell_0$  norm minimization for sparse reconstruction in compressed sensing. *Sensors*, 18(10):3373, 2018.
- Kishan Wimalawarne, Ryota Tomioka, and Masashi Sugiyama. Theoretical and experimental analyses of tensor-based regression and classification. *Neural computation*, 28(4):686–715, 2016.

- Yao Lei Xu, Kriton Konstantinidis, and Danilo P Mandic. Graph-regularized tensor regression: A domain-aware framework for interpretable multi-way financial modelling. *arXiv preprint arXiv:2211.05581*, 2022.
- Hua Zhou, Lexin Li, and Hongtu Zhu. Tensor regression with applications in neuroimaging data analysis. *Journal of the American Statistical Association*, 108(502):540–552, 2013.